

## A REVIEW ON MONITORING OF ATMOSPHERIC PARAMETERS FROM MICROWAVE RADIOMETER DATA USING LABVIEW™

Pallavi Asthana<sup>1</sup>, J.S.Pillai<sup>2</sup> and M.S.Panse<sup>1</sup>

<sup>1</sup>Veeramata Jijabai Technological Institute, Mumbai, India

<sup>2</sup>Society for Applied Microwave Electronics Engineering and Research, Mumbai, India

### ABSTRACT

Microwave Radiometer systems are used to monitor atmospheric temperature and humidity. Retrieving this atmospheric parameter from microwave radiometer measurement is an inverse problem, which cannot be solved without a solution to the forward problem. The forward problem consists of modelling the brightness temperature that an upward-looking microwave radiometer oriented at the specified elevation angle would observe, given predetermined radiosonde data. With the advent of the Microwave Radiometer, passive remote sensing of clouds and precipitation has become an indispensable tool in a variety of meteorological and oceanographical applications. In this paper, a general overview of physical fundamentals, measurement techniques, and retrieval methodology is given. This paper also describes the LabVIEW based software development to compute the brightness temperature ( $T_b$ ) for different frequencies band in the microwave region and for different heights. This  $T_b$  can be used for upward looking microwave radiometer system to compute the temperature and humidity by inversion problem. For the computation of  $T_b$ , weighting function has to be calculated first using Rayleigh approximation.

### I. INTRODUCTION

Microwave Radiometer measures energy emitted at sub-millimetre to centimetre wavelengths (at frequencies of 1-1000 GHz). The spatial as well as spectral characteristics of observed energy sources determine the performance requirements imposed on the functional subsystems of the sensors. These subsystems include an antenna, receiver and output indicator [12].

The power received by an antenna immersed in a blackbody at a temperature  $T_B$  is frequency independent and equivalent to the Johnson noise power that would be radiated by an antenna if it were terminated in a matched resistive load at the same temperature  $T$ .

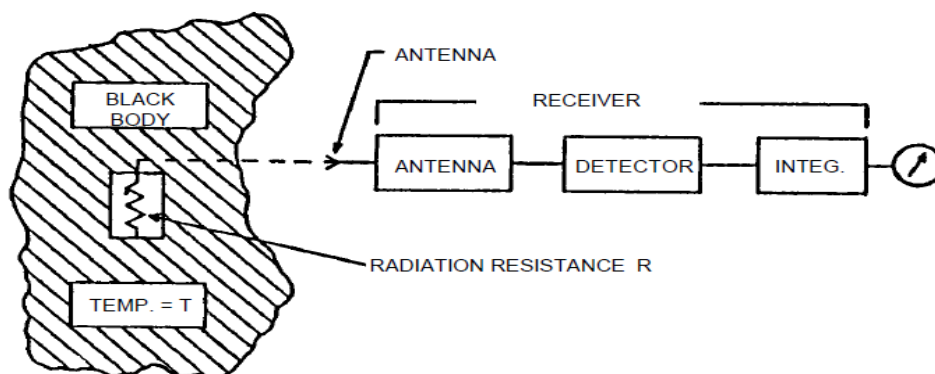


**Figure 1:** Simplified block diagram of an antenna and receiver. When the antenna is immersed in a blackbody at temperature  $T$ , the receiver input is equivalent to a resistive load  $R$  immersed in a thermal bath at temperature  $T$  [12]

These two fundamental sources of noise power are equivalent at microwave frequencies due to the inverse wavelength squared dependence of blackbody brightness, which is offset by the wavelength squared dependence of the antenna cross section. Hence, the noise power per unit cycle received by an antenna and presented at its output terminals is directly proportional to the effective blackbody temperature which characterizes the source or sources in which the antenna pattern is immersed. The proportionality factor is Boltzmann's constant ( $k$ ) [7].

As Microwave Radiometer systems are used to monitor atmospheric temperature and humidity. Retrieving this atmospheric parameter from microwave radiometer measurement is an inverse problem, which cannot be solved without a solution to the forward problem. The forward problem consists of modelling the brightness temperature from an upward-looking microwave radiometer oriented at the specified elevation angle would observe, given predetermined radiosonde data. A weighting function for a specific atmospheric parameter gives the theoretical change in radiometer  $T_B$  that results from a unit change in that parameter at a given height. The weighting functions are specific to the radiometer channel frequency and antenna orientation.

### 1.1 Microwave Absorption and Emission:

The principal sources of atmospheric microwave emission and absorption are water vapour, oxygen, and cloud liquid. In the frequency region from 20 to 200 GHz, water-vapour absorption arises from the weak electric dipole rotational transition at 22.235 GHz and the much stronger transition at 183.31 GHz. In addition, the so-called continuum absorption of water vapour arises from the far wing contributions from higher-frequency resonances that extend into the infrared region. Again, in the frequency band from 20 to 200 GHz, oxygen absorbs due to a series of magnetic dipole transitions centred around 60 GHz and the isolated line at 118.75 GHz. Because of pressure broadening, i.e., the effect of molecular collisions on radiative transitions, both water vapour and oxygen absorption extend outside of the immediate frequency region of their resonant lines. There are also resonances by ozone that are important for stratospheric sounding [5]. In addition to gaseous absorption, scattering, absorption, and emission also originate from hydrometeors in the atmosphere. Our focus in this article is on non-precipitating clouds for which emission and absorption are of primary importance.

## II. SYSTEM OVERVIEW

In the first step, forward problem is considered. Weighting function for temperature, pressure and water vapour is calculated, which is used for the calibration of brightness temperature using LabVIEW. Different models are available for the calculation of weighting functions. In **Ulaby** model, it mainly has 10 water vapour absorbing lines and 39 oxygen absorbing lines among 0-1000GHz, the smallest is 22.235GHz, and others are 183.31, 448.00 GHz. Oxygen microwave absorption spectrum is composed of many absorption lines distributed in the range of 50-70GHz (known as 60GHz oxygen line bundle) and 118.75GHz increasing spectrum line. And in respect to the ground-based microwave radiometer of 1-100 GHz, the mainly line is located at 22.235GHz and 50-60GHz.

In MPM model (atmospheric millimeter-wave propagation model), modular, quantitative relationships were developed between meteorological conditions encountered in the neutral atmosphere and corresponding refractivity. The contributions by water vapor and dry air and suspended water droplets such as cloud, fog, haze are reviewed. Compared to Ulaby model, it considers more elements and derives better results in precise simulation. The model mainly has 6 parts: local line absorption including water vapor and oxygen, no resonant dry air spectrum, water vapor continuum, suspended water droplet refractivity and rain effects. Because of the limitation of space, the equations of these 6 parts are not listed in detail. All of them can be find in reference [3]. Compared to Ulaby model, this MPM model has more considerations in the water vapor spectrum lines, like water vapor continuum, and suspended particles.

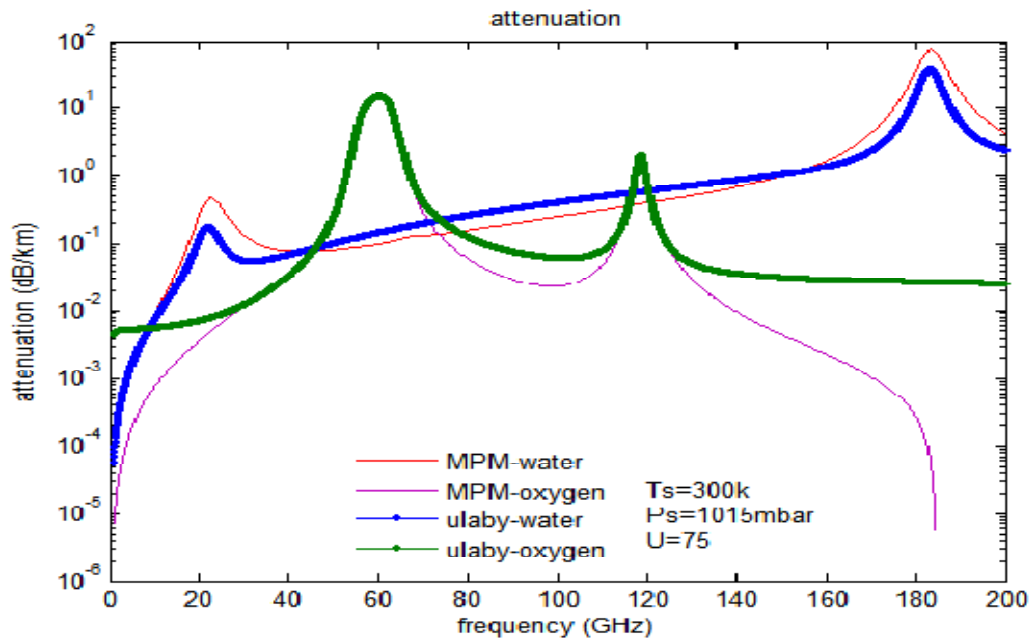


Figure 2. Comparison of Ulaby and MPM model[6]

LabVIEW is a graphical programming language that uses icons instead of lines of text to create applications. In contrast to text-based programming languages, where instructions determine the order of program execution, LabVIEW uses dataflow programming, where the flow of data through the nodes on the block diagram determines execution of virtual instrument and functions. It is Graphical User Interface (GUI) which in some way works as Human Machine Interface. Virtually, an instrument is designed in LabVIEW and one can acquire, analyze and process the data in the same way as an actual instrument can. Moreover, it has advantage of fast processing and high detection rate. Programs in LabVIEW are called Virtual Instruments (VIs), consists of a Block Diagram and a Front Panel. A Block Diagram provides a graphical code developments environment whereas a Front Panel allows the user to interact with a VI. It provides an efficient and easy-to-use environment for code development and makes program user friendly. It is more effective especially when the user needs to interact with the program and visualize the results. Unlike text-based programming languages like C and MATLAB which follow a control flow execution model, the environment of programming follows a dataflow execution model [10-11]. Figure 3 shows the block diagram of the Scheme.

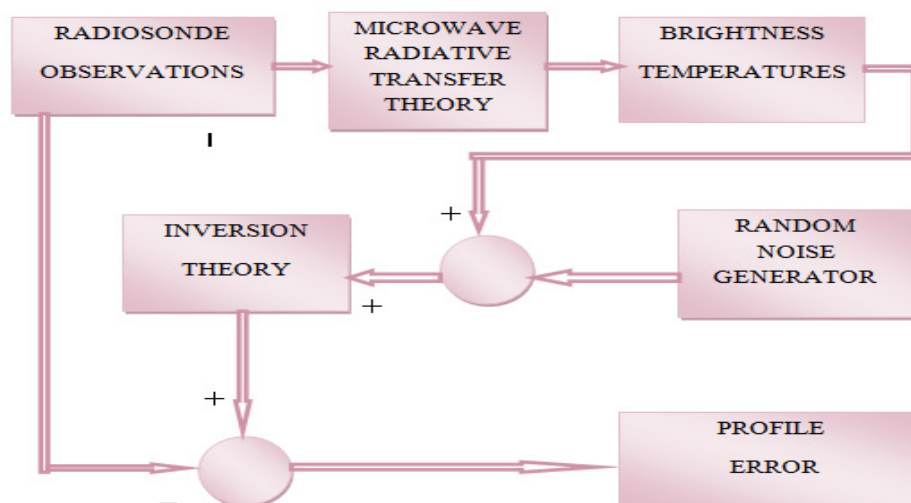


Figure 3. Block diagram of the scheme.

**Defining Brightness Temperature ( $T_B$ ):**

From the concept of an ideal black body and Kirchoff's law, it is known that the emission from a black body depends only on its temperature and that the higher the temperature of the body, the more is its emission. The idea is made quantitative by calculating the spectral distribution of a blackbody emission from Planck's law, which expresses the radiance  $B_\nu(T)$  emitted from a blackbody at temperature  $T$  and frequency  $\nu$  as

$$B_\nu(T) = \frac{2h\nu^3}{c^2} \frac{1}{\left(\exp\left(\frac{h\nu}{kT}\right) - 1\right)}$$

Where,  $h$  = Planck's constant, and  $k$  = Boltzmann's constant. The radiance expresses the emitted power per unit projected area per unit solid angle per unit frequency interval. The second consideration is to relate the emission from a real body, sometimes called a "grey" body, to that of a blackbody at the same temperature. If the fraction of incident energy from a certain direction absorbed by the grey body is  $A(\nu)$ , then the amount emitted is  $A(\nu) B_\nu(T)$ . For a perfectly reflecting or transmitting body,  $A(\nu)$  is zero, and incident energy may be redirected or pass through the body without being absorbed. In the situation considered here, namely upward-looking radiometers viewing a non-scattering medium, the equation that relates our primary observable, brightness temperature,  $T_B$ , to the atmospheric state is the radiative transfer equation (RTE) [6]

$$B_\nu(T_b) = B_\nu(T_c) \exp(-\tau_\nu) + \int_0^\infty B_\nu(T(s)) \alpha_\nu(s) \exp\left(-\int_0^s \alpha_\nu(s') ds'\right) ds$$

Where,  $s$  = path length in km,  $T(s)$  = Temperature (K) at the point  $s$ ,  $T_c$  = Cosmic background brightness temperature of 2.75 K,  $\tau_\nu$  = opacity = total optical depth along the path.

$$\tau_\nu = \int_0^\infty \alpha_\nu(s) ds$$

Where,  $\alpha_\nu(s)$  = absorption coefficient (nepers/km) at the point  $s$ . The use of the blackbody source function is justified by the assumption of local thermodynamic equilibrium in which the population of emitting energy states is determined by molecular collisions and is independent of the incident radiation field [6].

**III. RADIOMETRIC RESPONSE TO ATMOSPHERIC PROFILES: WEIGHTING FUNCTIONS**

Equations (2) describe the theoretical radiometric response to atmospheric temperature  $T(s)$  and absorption coefficient  $\alpha_\nu(s)$  as a function of the path coordinate  $s$ . The absorption coefficient, in turn, is a function of  $T(s)$ , pressure  $P(s)$ , water vapour density  $\rho_\nu(s)$ , and cloud liquid density  $\rho_L(s)$ . We are assuming conditions for which the Rayleigh approximation is valid. In general, the response  $B_\nu(T_B)$  to profiles is a nonlinear function of  $T$ ,  $P$ ,  $\rho_\nu$  and  $\rho_L$  i.e.  $B_\nu = B_\nu\{T, P, \rho_\nu, \rho_L\}$ .

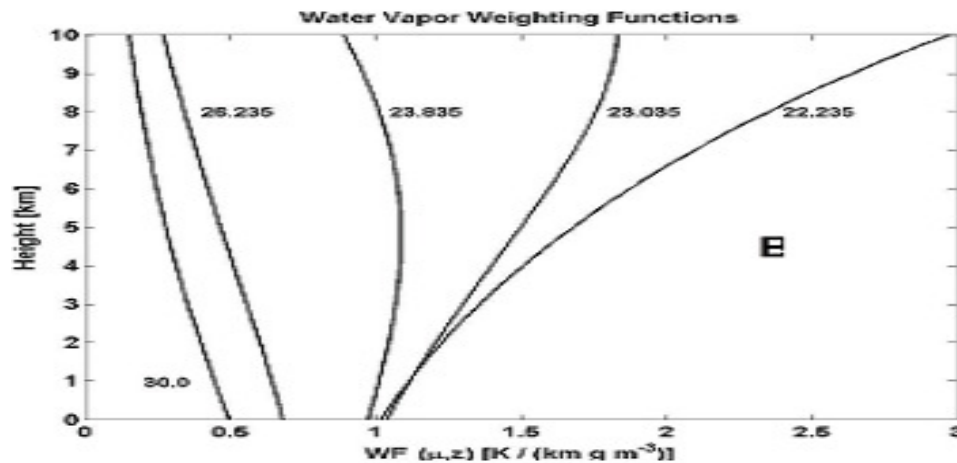


Figure 4. Humidity weighting function[6]

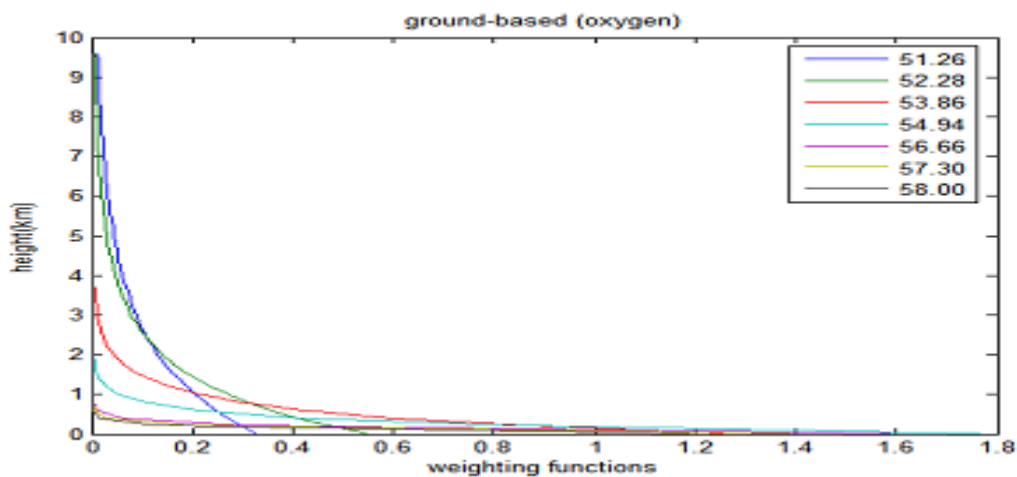


Figure 5. Temperature weighting function[6]

#### IV. RETRIEVAL TECHNIQUES

Techniques to derive meteorological information from radiation measurements are generally based on its perturbation form. Because only a finite number of imperfect radiation measurements are available, and a continuum of parameters is needed to describe profiles of temperature, water vapor, and cloud liquid, a rigorous mathematical solution does not exist and the inverse problem is said to be ill-posed. Therefore, it is better to regard the measurements as constraints and to blend them with supplementary sources of information or to drastically reduce the dimensionality of the inverse problem by projecting the profiles onto their linear functionals. Useful supplementary information can be provided by numerical meteorological forecasts, or by a priori information obtained from past data. Examples of profile linear functionals are PWV and LWP for moisture variables and geopotential height for temperature profiles.

#### V. RESULT AND CONCLUSION

We have developed the algorithm and calculate the absorption coefficient of atmosphere according to ULABY Model, and the software being developed for the computation of brightness temperature from radiosonde data using LabVIEW™. This technique primary used for ground based microwave radiometer in the two frequency bands, namely 20-30 GHz and 50-60 GHz, with multiple channels in each band.

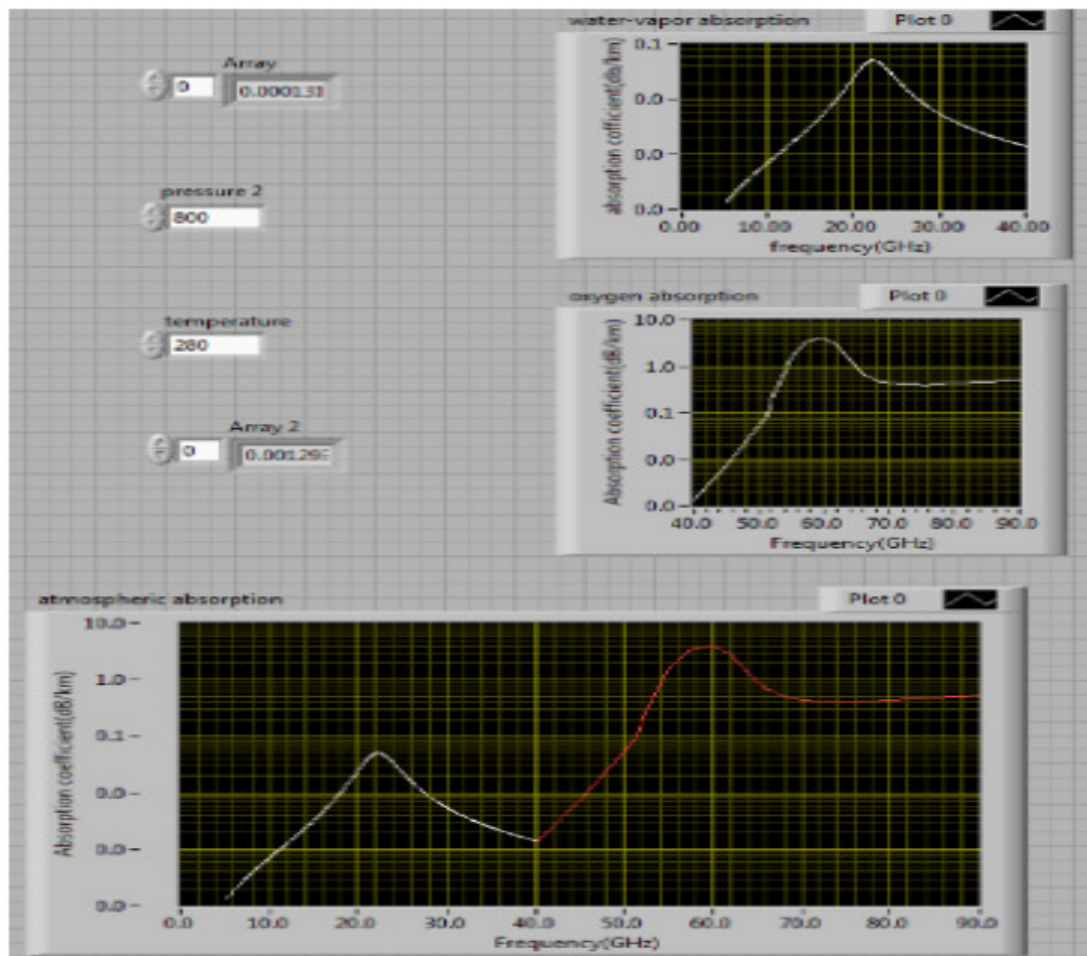


**Figure 6:** Absorption coefficient using Ulaby Model

The model is used to compute the radiative properties of atmospheric gases (here water vapour and oxygen). The development of parametric radiative transfer model with the detailed description of all the atmospheric quantities is the key in the inverse model construction.

## REFERENCES

- [1] Gordon Farquharson, Eric Loew, Jothiram Vivekanandan, and Wen-Chau Lee, "A New High-Altitude Airborne Millimeter-Wave Radar for Atmospheric Research," *IEEE*, pp 3313-3316, sep 2007.
- [2] H. J. Liebe, G.A. Hufford, M. G. Cotton, "Propagation Modeling of Moist Air and Suspended Water/ice Particles at Frequencies Below 1000 GHz," *Proc. Of Atmospheric propagation effects through natural and man-made observant for visible to MM-wave radiation*, pp 3.1-3.10, may 1993.
- [3] LiLi, J. Vivekanadan, C.H. Chan, and Leung Tsang, "Microwave Radiometric technique to retrieve vapour, liquid and ice, part I- Development of a Neutral Network based inversion method," *Int J of Infrared and Millimeter Waves*, vol35, pp 224-235, 2<sup>nd</sup> march 1992.
- [4] Jan I. H. Askne, and ED R. Westwater, "A review of ground-based remote sensing of temperature and moisture by passive Microwave Radiometer," *IEEE transactions on geosciences and remote sensing*, vol24, pp 340-352, 3<sup>rd</sup> may 1986.
- [5] Ed R. Westwater, Susanne Crewell, Christian Mätzler, and Domenico Cimini, "Principles of Surface-based Microwave and Millimeter wave Radiometric Remote Sensing of the Troposphere," *international union of radio-science*, vol301, pp 59-80, sep 2004.
- [6] Jieying He, Shengwei Zhang, Yu Zhang, Fenglin Sun, "The Analysis of Atmospheric Absorption Model Based on Ground-based Microwave Radiometer," *Proceedings of International Symposium on Signals, Systems and Electronics*, vol35, pp 40-44, 10<sup>th</sup> sep 2010.

- [7] ED R. Westwater, Jack B. Snider, and Michael J. Falls, "Ground-Based Radiometric Observations of Atmospheric Emission and Attenuation at 20.6, 31.65, and 90.0 GHz: A Comparison of Measurements and Theory," *IEEE Transactions on antennas and propagation*, vol.38, pp 1569-1579 10<sup>th</sup> oct 1990.
- [8] LabVIEW User Manual from National Instruments.
- [9] Virtual Instrumentation Using LabVIEW, by Sanjay Gupta and Joseph John, Tata McGraw-Hill companies.
- [10] Trevis (e-book), "LabVIEW for Everyone Graphical Programming," Made Easy Fun, third edition.
- [11] [www.ni.com](http://www.ni.com)
- [12] <http://www.radiometric.com>

**Pallavi Asthana** received her B.Tech. degree from the Electronics & Instrumentation Eng. Department, SGSITS, Indore in 2009. At present she is pursuing her M.Tech. degree with VJTI, Mumbai. Her research interests are ground based microwave radiometer and sodar applications.



**M. S. Panse** is working as a senior professor of Electronics Engineering at VJTI, Mumbai. She has over 25 years of teaching and research experience. She has 81 international and national level publications to her credit. Her research interests include Biomedical Engineering-prosthetic devices, application of virtual instrumentation etc.



**J S Pillai** received M.Tech in Solid State Technology from IIT, Madras in 1987. He has been working in the field of development of atmospheric instrumentation including SODAR, wind profiler, RASS and Microwave Radiometer. His field of interest includes atmospheric instrumentation, virtual instrumentation, signal processing and data processing. He has more than 25 publications in various national, international journals and proceeding of symposia.

